

# Geometric Factors in Target Positioning and Tracking

Chun Yang  
Sigtem Technology, Inc.  
San Mateo, CA 94402  
[chunynag@sigtem.com](mailto:chunynag@sigtem.com)

Erik Blasch  
Air Force Research Lab  
WPAFB, OH 45433  
[erik.blasch@wpafb.afb.mil](mailto:erik.blasch@wpafb.afb.mil)

Ivan Kadar  
Interlink Sciences Systems, Inc.  
Lake Success, NY 11042  
[ikadar@SystemsSciences.com](mailto:ikadar@SystemsSciences.com)

**Abstract** - *In target positioning and tracking, most sensors provide measurements either as range or bearing or both. The measurements are used to update an a priori estimate either via a linearized least squares method or an extended Kalman filter. In either case, the resulting solution has two components, one is related to the measurement prediction errors and the other is an observation matrix obtained from linearizing the nonlinear measurement equations around the a priori estimate. This paper studies the geometric factors explicitly and relates the observation matrix to the line of sight (LOS) vector for a ranging sensor and the direction perpendicular to the LOS vector of a bearing-only sensor. As a result, the updating of estimation error covariance with range and bearing measurements can be intuitively assessed via the shaping of estimation error ellipse along LOS directions. It provides a valuable means for target positioning and tracking performance modeling and prediction and can thus be used in active management of distributed sensor resources and sensor path planning.*

**Keywords:** Ranging & Bearing-Only Sensors, Geometry, LOS, GDOP.

## 1 Introduction

Passive and active sensors are widely used in target position location and tracking [1, 2, 3, 7, 10]. Passive sensors include (1) acoustic sensors that detect ground vehicle motion and vibration and (2) imaging sensors that capture reflected visible lights or radiated thermal energy from a target. In addition to signatures characteristic to targets for possible identification, these passive sensors also measure the direction of arrival of the mechanic or electromagnetic signals of the targets in terms of their bearing angles relative to the sensor platforms for positioning and tracking. Additional examples include passive sonar sensors for underwater applications and passive radar sensors for space observations [8].

Active sensors include radar, laser radar, and active sonar. By measuring the round trip time of flight of an energy pulse, active sensors provide range measurements to targets. Time difference of arrival (TDOA) is a common technique for differential range calculations. Some active sensors also measure the angles of arrival (AOA) of returned pulse or the direction in which the transmit beam is pointed. Monopulse and antenna array techniques provide more accurate angular measurements than mechanically scanned antennas. Other active sensors are capable of extracting the Doppler frequency shifts impacted by target motion, thus measuring the range rate.

According to the type of measurements, most sensors used in target positioning and tracking can be viewed as measuring either range or bearing or both (without considering range rate and target signature measurements) [10]. A target's position is determined using multilateration with ranging sensors or triangulation with angular sensors or their mixture. Multilateration or triangulation can be done when a target is viewed by multiple distributed sensors or by a single sensor moving along (multiple views). A batch processing mode may use the conventional least squares (LS) method whereas a sequential processing mode calls for the Kalman filter [1, 2, 3, 7, 10].

Indeed, the sensor measurements are used to update an *a priori* estimate either via a linearized least squares method or an extended Kalman filter. In either case, the resulting solution has two components, one is related to the *measurement prediction errors* and the other is an *observation matrix* obtained from linearizing the nonlinear measurement equations around the *a priori* estimate. The observation matrix, which determines the estimation error covariance, has a distinct structure containing the geometric information for a given target positioning and tracking setting.

It is well known that the observation matrix is related to the sensing geometry. However, this paper elucidates the geometric factors for both active and passive sensors [4, 14, 15] and explicitly relates the observation matrix to the line of sight (LOS) vector for a ranging sensor and the direction perpendicular to the LOS vector of a bearing-only sensor. The geometric expression provides a mathematical basis for the well-known fact that the error ellipses for co-located passive and ranging sensors are perpendicular.

Furthermore, the updating of estimation error covariance (i.e., the eigen structure) with range and bearing measurements can be intuitively assessed via the shaping of estimation error ellipse along LOS directions. For an anticipated tracking scenario, this provides an efficient means for target positioning and tracking performance modeling and prediction and can thus be used in active management of distributed sensor resources and sensor path planning [5, 6, 9, 16].

The rest of the paper is organized as follows. In Section 2, the least squares method is used to relate the position solution to the observation matrix and to the LOS vectors. In Section 3, the updating of error covariance by LOS vectors is characterized with simulation examples. Finally, the paper is concluded in Section 4.

# Report Documentation Page

Form Approved  
OMB No. 0704-0188

Public reporting burden for the collection of information is estimated to average 1 hour per response, including the time for reviewing instructions, searching existing data sources, gathering and maintaining the data needed, and completing and reviewing the collection of information. Send comments regarding this burden estimate or any other aspect of this collection of information, including suggestions for reducing this burden, to Washington Headquarters Services, Directorate for Information Operations and Reports, 1215 Jefferson Davis Highway, Suite 1204, Arlington VA 22202-4302. Respondents should be aware that notwithstanding any other provision of law, no person shall be subject to a penalty for failing to comply with a collection of information if it does not display a currently valid OMB control number.

1. REPORT DATE <b>JUL 2009</b>		2. REPORT TYPE		3. DATES COVERED <b>06-07-2009 to 09-07-2009</b>	
4. TITLE AND SUBTITLE <b>Geometric Factors in Target Positioning and Tracking</b>				5a. CONTRACT NUMBER	
				5b. GRANT NUMBER	
				5c. PROGRAM ELEMENT NUMBER	
6. AUTHOR(S)				5d. PROJECT NUMBER	
				5e. TASK NUMBER	
				5f. WORK UNIT NUMBER	
7. PERFORMING ORGANIZATION NAME(S) AND ADDRESS(ES) <b>Sigten Technology, Inc., , San Matero, CA, 94402</b>				8. PERFORMING ORGANIZATION REPORT NUMBER	
9. SPONSORING/MONITORING AGENCY NAME(S) AND ADDRESS(ES)				10. SPONSOR/MONITOR'S ACRONYM(S)	
				11. SPONSOR/MONITOR'S REPORT NUMBER(S)	
12. DISTRIBUTION/AVAILABILITY STATEMENT <b>Approved for public release; distribution unlimited</b>					
13. SUPPLEMENTARY NOTES <b>See also ADM002299. Presented at the International Conference on Information Fusion (12th) (Fusion 2009). Held in Seattle, Washington, on 6-9 July 2009. U.S. Government or Federal Rights License.</b>					
14. ABSTRACT <b>In target positioning and tracking, most sensors provide measurements either as range or bearing or both. The measurements are used to update an a priori estimate either via a linearized least squares method or an extended Kalman filter. In either case, the resulting solution has two components, one is related to the measurement prediction errors and the other is an observation matrix obtained from linearizing the nonlinear measurement equations around the a priori estimate. This paper studies the geometric factors explicitly and relates the observation matrix to the line of sight (LOS) vector for a ranging sensor and the direction perpendicular to the LOS vector of a bearing-only sensor. As a result, the updating of estimation error covariance with range and bearing measurements can be intuitively assessed via the shaping of estimation error ellipse along LOS directions. It provides a valuable means for target positioning and tracking performance modeling and prediction and can thus be used in active management of distributed sensor resources and sensor path planning.</b>					
15. SUBJECT TERMS					
16. SECURITY CLASSIFICATION OF:			17. LIMITATION OF ABSTRACT <b>Public Release</b>	18. NUMBER OF PAGES <b>8</b>	19a. NAME OF RESPONSIBLE PERSON
a. REPORT <b>unclassified</b>	b. ABSTRACT <b>unclassified</b>	c. THIS PAGE <b>unclassified</b>			

## 2 Geometric Scaling via LOS Vectors

In this section, we first present the position solution via the least squares method. We then relate it to the observation matrix via linearization. Next we express the observation matrix in terms of LOS vector for active and passive sensors.

### 2.1 Least Squares Solutions

Consider a target at  $\mathbf{x}$  and the  $i$ -th sensor at  $\mathbf{x}_i$ . The  $i$ -th sensor's measurement is given by:

$$z_i = f_i(\mathbf{x}, \mathbf{x}_i) + v_i \quad (1)$$

where  $f_i(\cdot, \cdot)$  is a nonlinear measurement equation and  $v_i$  is the sensor measurement error being zero-mean Gaussian  $\mathcal{N}(0, \sigma_i^2)$ .

Denote an initial estimate of the target state by  $\mathbf{x}_0$ . The nonlinear measurement, be a range or a bearing, can be linearized around the estimate:

$$z_i \approx f_i(\mathbf{x}_0, \mathbf{x}_i) + \mathbf{h}_i^T (\mathbf{x} - \mathbf{x}_0) + v_i \quad (2a)$$

$$\mathbf{h}_i^T = \begin{bmatrix} \frac{\partial z_i}{\partial x_1} & \frac{\partial z_i}{\partial x_2} & \dots & \frac{\partial z_i}{\partial x_n} \end{bmatrix} \quad (2b)$$

In terms of measurement prediction error, the equation can be further written as:

$$\tilde{z}_i = z_i - f_i(\mathbf{x}_0, \mathbf{x}_i) + \mathbf{h}_i^T \mathbf{x}_0 = \mathbf{h}_i^T \mathbf{x} + v_i \quad (3)$$

For  $m$  sensors, the linearized measurements can be put into a vector format as:

$$\tilde{\mathbf{z}} = \mathbf{H}\mathbf{x} + \mathbf{v} \quad (4a)$$

$$\tilde{\mathbf{z}}^T = [\tilde{z}_1 \quad \tilde{z}_2 \quad \dots \quad \tilde{z}_m] \quad (4b)$$

$$\mathbf{v}^T = [v_1 \quad v_2 \quad \dots \quad v_m] \quad (4c)$$

$$\mathbf{H}^T = [\mathbf{h}_1 \quad \dots \quad \mathbf{h}_m] \quad (4d)$$

An estimate of the target state given the measurements can be obtained as the least squares (LS) solution to the following performance index as:

$$\hat{\mathbf{x}} = \arg \min_{\mathbf{x}} (\tilde{\mathbf{z}} - \mathbf{H}\mathbf{x})^T \mathbf{R}^{-1} (\tilde{\mathbf{z}} - \mathbf{H}\mathbf{x}) \quad (5a)$$

where  $\mathbf{R}$  is the measurement noise covariance matrix defined as:

$$\mathbf{R} = E\{\mathbf{v}\mathbf{v}^T\} \quad (5b)$$

The least square solution is given by:

$$\hat{\mathbf{x}} = (\mathbf{H}^T \mathbf{R}^{-1} \mathbf{H})^{-1} \mathbf{H}^T \mathbf{R}^{-1} \tilde{\mathbf{z}} \quad (6a)$$

$$\mathbf{P} = E\{(\mathbf{x} - \hat{\mathbf{x}})^T (\mathbf{x} - \hat{\mathbf{x}})\} = (\mathbf{H}^T \mathbf{R}^{-1} \mathbf{H})^{-1} \quad (6b)$$

Assume that, in addition to the initial estimate of the target state  $\mathbf{x}_0$ , the estimation error covariance, denoted by  $\mathbf{P}_0$ , is also known. Then, given the target measurements as in (4a), we can obtain the weighted least square (WLS) solution that minimizes the following performance index as:

$$\hat{\mathbf{x}} = \arg \min_{\mathbf{x}} (\tilde{\mathbf{z}} - \mathbf{H}\mathbf{x})^T \mathbf{R}^{-1} (\tilde{\mathbf{z}} - \mathbf{H}\mathbf{x}) + (\mathbf{x} - \mathbf{x}_0)^T \mathbf{P}_0^{-1} (\mathbf{x} - \mathbf{x}_0) \quad (7)$$

The least squares solution is given by:

$$\hat{\mathbf{x}} = (\mathbf{H}^T \mathbf{R}^{-1} \mathbf{H} + \mathbf{P}_0^{-1})^{-1} (\mathbf{H}^T \mathbf{R}^{-1} \tilde{\mathbf{z}} + \mathbf{P}_0^{-1} \mathbf{x}_0) \quad (8a)$$

$$\mathbf{P} = (\mathbf{H}^T \mathbf{R}^{-1} \mathbf{H} + \mathbf{P}_0^{-1})^{-1} \quad (8b)$$

Alternatively, we can treat the *a priori* knowledge  $\mathbf{x}_0$  and  $\mathbf{P}_0$  as an additional measurement and obtain the augmented measurement equations as:

$$\tilde{\mathbf{z}} = \mathbf{H}\mathbf{x} + \mathbf{v} \quad (9a)$$

$$\mathbf{x}_0 = \mathbf{x} + \boldsymbol{\varepsilon} \quad (9b)$$

$$\mathbf{v} \sim \mathcal{N}(\mathbf{0}, \mathbf{R}), \boldsymbol{\varepsilon} \sim \mathcal{N}(\mathbf{0}, \mathbf{P}_0), E\{\mathbf{v}\boldsymbol{\varepsilon}^T\} = \mathbf{0} \quad (9c)$$

Now apply the Kalman filter's measurement updating step to the augmented measurement  $[\tilde{\mathbf{z}}^T \quad \mathbf{x}_0^T]^T$  as:

$$\hat{\mathbf{x}} = \left( \begin{bmatrix} \mathbf{H}^T & \mathbf{I} \end{bmatrix} \begin{bmatrix} \mathbf{R}^{-1} & \mathbf{0} \\ \mathbf{0} & \mathbf{P}_0^{-1} \end{bmatrix} \begin{bmatrix} \mathbf{H} \\ \mathbf{I} \end{bmatrix} \right)^{-1} \begin{bmatrix} \mathbf{H}^T & \mathbf{I} \end{bmatrix} \begin{bmatrix} \mathbf{R}^{-1} & \mathbf{0} \\ \mathbf{0} & \mathbf{P}_0^{-1} \end{bmatrix} \begin{bmatrix} \tilde{\mathbf{z}} \\ \mathbf{x}_0 \end{bmatrix} \quad (10)$$

The terms in front of  $[\tilde{\mathbf{z}}^T \quad \mathbf{x}_0^T]^T$  in (10) constitute the Kalman filter gain. Expanding the matrices in terms of their elements leads to the solution (8a). Similarly, the Kalman filter's covariance updating step can be written up for the augmented equations, leading to the updated covariance (8b). Note that the inverse of the covariance matrix in (8b) is also called the *information matrix*, denoted by  $\boldsymbol{\Lambda}$ :

$$\boldsymbol{\Lambda} = \mathbf{P}^{-1} = \mathbf{H}^T \mathbf{R}^{-1} \mathbf{H} + \mathbf{P}_0^{-1} \quad (11)$$

### 2.2 Active Ranging Sensors

First consider the case with active sensors (ranging measurements) in a two dimensional setting. The nonlinear range equation (1) is spelled out as (ignore the noise term):

$$r_i = f_i(\mathbf{x}, \mathbf{x}_i) = \sqrt{(x - x_i)^2 + (y - y_i)^2} \quad (12a)$$

The corresponding linearized equation around an initial estimate  $\mathbf{x}_0$  of  $\mathbf{x}$  is:

$$r_i \approx f_i(\mathbf{x}_0, \mathbf{x}_i) + \mathbf{h}_i^T (\mathbf{x} - \mathbf{x}_0) \quad (12b)$$

with

$$\mathbf{h}_i = \begin{bmatrix} x_0 - x_i \\ r_i \\ y_0 - y_i \\ r_i \end{bmatrix} = \begin{bmatrix} \cos(\theta_i) \\ \sin(\theta_i) \end{bmatrix} = \mathbf{e}_i \quad (12c)$$

It is clear from (12b) that  $\mathbf{h}_i$  is the line of sight (LOS) vector from the  $i$ -th sensor to the target, denoted by  $\mathbf{e}_i$ , as shown in Fig. 1.

### 2.3 Passive Bearing-Only Sensors

Referring to Fig. 1, we now consider the case with passive sensors (bearing measurements) still in a two dimensional setting.

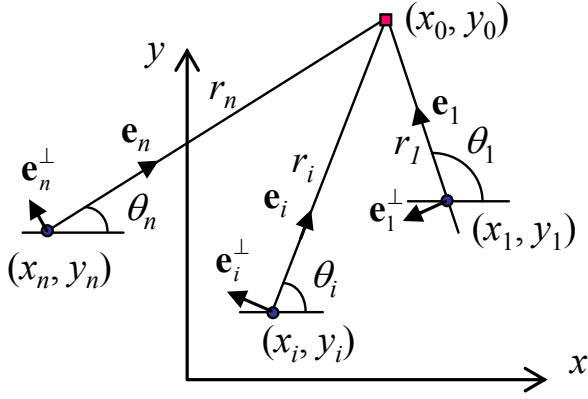


Fig. 1 Ranging and Bearing-Only Sensors

The nonlinear angular equation is:

$$f_i(\mathbf{x}, \mathbf{x}_i) = \theta_i = \tan^{-1}\left(\frac{y - y_i}{x - x_i}\right) \quad (13a)$$

which can be linearized around an initial estimate  $\mathbf{x}_0$  of  $\mathbf{x}$  as:

$$\theta_i \approx f_i(\mathbf{x}_0, \mathbf{x}_i) + \mathbf{h}_i^T (\mathbf{x} - \mathbf{x}_0) \quad (13b)$$

where

$$\mathbf{h}_i = \begin{bmatrix} -\frac{y_0 - y_i}{r_i^2} \\ \frac{x_0 - x_i}{r_i^2} \end{bmatrix} = \begin{bmatrix} -\sin(\theta_i) \\ \cos(\theta_i) \end{bmatrix} = \frac{1}{r_i} \begin{bmatrix} -\sin(\theta_i) \\ \cos(\theta_i) \end{bmatrix} = \frac{\mathbf{e}_i^\perp}{r_i} \quad (13c)$$

Comparing (13c) to (12c), it shows that the measurement matrix  $\mathbf{h}_i$  for the bearing-only sensor is range-dependent. More importantly, it is perpendicular to the line of sight vector from sensor to target. When the range-dependence and angular errors are combined, it provides a position error of  $r_i \sigma_i$  along the direction perpendicular to the LOS (i.e., along  $\mathbf{e}_i^\perp$ ).

## 2.4 Geometric Dilution of Precision (GDOP)

A scalar value that characterizes the position solution is the geometrical dilution of precision (GDOP) defined as [4, 13]:

$$\text{GDOP} = \sqrt{\text{trace}(\mathbf{H}^T \mathbf{R}^{-1} \mathbf{H})^{-1}} \quad (14a)$$

$$= \sqrt{\text{trace}(\mathbf{H}^T \mathbf{H})^{-1}} \quad \text{when } \mathbf{R} = \mathbf{I} \quad (14b)$$

For the case with two ranging sensors, the GDOP can be written as:

$$\text{GDOP}_{\text{Range}} = \sqrt{\frac{\sigma_1^2 + \sigma_2^2}{\sin^2(\theta_1 - \theta_2)}} \quad (15a)$$

$$= \begin{cases} \sqrt{\sigma_1^2 + \sigma_2^2}, & |\theta_1 - \theta_2| = \pi/2 \\ \infty, & |\theta_1 - \theta_2| = 0, \pi \end{cases} \quad (15b)$$

For the case with two bearing-only sensors, the GDOP can be written as:

$$\text{GDOP}_{\text{Bearing}} = \sqrt{\frac{r_1^2 \sigma_1^2 + r_2^2 \sigma_2^2}{\sin^2(\theta_1 - \theta_2)}} \quad (16a)$$

$$= \begin{cases} \sqrt{r_1^2 \sigma_1^2 + r_2^2 \sigma_2^2}, & |\theta_1 - \theta_2| = \pi/2 \\ \infty, & |\theta_1 - \theta_2| = 0, \pi \end{cases} \quad (16b)$$

Eqs. (15) and (16) are consistent with our intuition that two perpendicular sensors can produce the best estimate and two collinear sensors cannot produce a solution. Different from ranging sensors, however, bearing-only sensors have range terms explicitly as in (13c). In fact, the error ellipses for passive and ranging sensors are perpendicular are well known. It is meaningful to explicitly show it from the observation matrix in terms of LOS vectors.

As shown next, the line of sight vectors and measurement error covariance matrices are related to the eigenvalues and eigenvector directions of the estimation error ellipses. When used to update a position solution, they shape the error ellipses by adjusting its size and orientation via the eigenstructure.

## 3 LOS Updating and Characterization

As shown in the last section, the linearized measurement equation for an active ranging sensor or a passive bearing-only sensor is characterized by (1) the line of sight (LOS) vector or its perpendicular and (2) the measurement error variance. A position solution is also determined by these two factors as is evident from the following equation of estimation error covariance:

$$\mathbf{P} = (\mathbf{H}^T \mathbf{R}^{-1} \mathbf{H} + \mathbf{P}_0^{-1})^{-1} \quad (17)$$

where  $\mathbf{P}_0$  is the a priori covariance matrix,  $\mathbf{P}$  is the a posteriori covariance matrix,  $\mathbf{H}$  is the measurement matrix, and  $\mathbf{R}$  is the measurement error covariance.

To simplify the analysis, first consider the case where  $\mathbf{P}_0 = \mathbf{I}$ ,  $\mathbf{H} = \mathbf{a}^T = [\cos \theta, \sin \theta]$ , which is a row vector with  $\theta$  being the angle relative to the  $x$ -axis, and  $\mathbf{R} = \sigma^2$ . This represents the case where the a priori estimate is updated by a single measurement. The updated covariance is given by:

$$(\mathbf{H}^T \mathbf{R}^{-1} \mathbf{H} + \mathbf{P}_0^{-1})^{-1} = (\mathbf{I} + \sigma^{-2} \mathbf{a} \mathbf{a}^T)^{-1} = \mathbf{I} - \gamma \mathbf{a} \mathbf{a}^T \quad (18a)$$

where

$$\gamma = \frac{1}{\mathbf{a}^T \mathbf{a} + \sigma^2} = \frac{1}{1 + \sigma^2} = \begin{cases} 1, & \sigma = 0 \\ 0, & \sigma = \infty \end{cases} \quad (18b)$$

It is easy to verify that  $\mathbf{a}$  is an eigenvector of the matrix  $(\mathbf{I} - \gamma \mathbf{a} \mathbf{a}^T)$  with the corresponding eigenvalue  $(1 - \gamma \mathbf{a}^T \mathbf{a}) = 1 - \gamma$ . For the 2D case, the other eigenvector is perpendicular to  $\mathbf{a}$ , denoted by  $\mathbf{a}^\perp$ , with the corresponding eigenvalue being unity.

In terms of geometry interpretation, the unity circle is shaped into an ellipse with the following eigenvalues and eigenvectors:

$$\mathbf{\Lambda} = \text{diag}([1 - \gamma \quad 1]) \quad (19a)$$

$$\mathbf{V} = [\mathbf{a} \quad \mathbf{a}^\perp] = \begin{bmatrix} a_1 & -a_2 \\ a_2 & a_1 \end{bmatrix} = \begin{bmatrix} \cos \theta & -\sin \theta \\ \sin \theta & \cos \theta \end{bmatrix} \quad (19b)$$

The following simulation is used to illustrate the characteristics of LOS updating. Let the initial covariance be a unit matrix,  $\mathbf{P}_0 = \text{diag}([1, 1])$ , which represents a circular error as shown in Fig. 2. We vary the LOS vector's orientation  $\theta$  relative to the  $x$ -axis and the measurement error covariance  $\mathbf{R} = \sigma^2$ . Fig. 2 shows two updates at  $(\theta, \sigma) = (30^\circ, 1)$  and  $(70^\circ, 0.5)$ , respectively. Each LOS update squeezes the circle into an ellipse with different orientation and different eccentricity. The orientation is such that the eigenvector corresponding to the small eigenvalue points along the LOS direction.

Fig. 3 shows eigenvector constriction where the major and minor eigenvectors are off by  $90^\circ$  as expected and the minor eigenvector's angle  $\phi$  changes linearly as the LOS angle  $\theta$ .

The major eigenvalue remains constant but the minor eigenvalue changes inversely with  $\sigma$  (according to (15b)) as shown in Fig. 4. The better the sensor performance (the smaller  $\sigma$ ), the smaller is the minor eigenvalue after update and vice versa.

If a sensor stares at a target in the same direction, the error ellipse is updated repeatedly by the same LOS vector (assume the target is not moving). Then the reduction of the minor eigenvalue over time (i.e., the number of updates) is shown in Fig. 5 for different sensor quality (i.e.,  $\mathbf{R}$ ). This is equivalent to time averaging.

For a single sensor, another way to reduce the errors in target positioning is to circle the target as in a spot synthetic aperture radar (SAR) operation. Update in one direction squeezes the error in that direction. When it is done in all directions, it makes a smaller error circle as shown Fig. 6 where the errors at 5 discrete angles are shown together with the initial large circle.

Fig. 7 shows the reduction of the eigenvalues as a function of LOS angle  $\theta$ . As shown, the major eigenvalue decreases rather quickly over the first  $90^\circ$  and then much slowly for next  $90^\circ$  and does not change much for the remaining  $180^\circ$ . This indicates that a single ranging sensor can significantly reduce positioning error by circling the target by  $90^\circ$  or so, which is consistent with our intuition and can be used as a practical guideline in sensor placement and scheduling.

Consider the case with two LOS updates simultaneously. The two sensors have their LOS vectors  $\mathbf{a}_1^T = [\cos \theta_1, \sin \theta_1]$  and  $\mathbf{a}_2^T = [\cos \theta_2, \sin \theta_2]$  with  $\sigma_1^2$  and  $\sigma_2^2$ , respectively. The updated covariance is given by [8]:

$$(\mathbf{I} + \sigma_1^{-2} \mathbf{a}_1 \mathbf{a}_1^T + \sigma_2^{-2} \mathbf{a}_2 \mathbf{a}_2^T)^{-1} = \mathbf{I} - \gamma(\gamma_1 \mathbf{a}_1 \mathbf{a}_1^T + \gamma_2 \mathbf{a}_2 \mathbf{a}_2^T - \rho \gamma_1 \gamma_2 \mathbf{a}_1 \mathbf{a}_2^T - \rho \gamma_1 \gamma_2 \mathbf{a}_2 \mathbf{a}_1^T) \quad (20a)$$

where

$$\rho = \mathbf{a}_1^T \mathbf{a}_2 \quad (20b)$$

$$\gamma_1 = \frac{1}{\sigma_1^2 + \mathbf{a}_1^T \mathbf{a}_1} = \frac{1}{\sigma_1^2 + 1} \quad (20c)$$

$$\gamma_2 = \frac{1}{\sigma_2^2 + \mathbf{a}_2^T \mathbf{a}_2} = \frac{1}{\sigma_2^2 + 1} \quad (20d)$$

$$\gamma = \frac{1}{1 - \rho^2 \gamma_1 \gamma_2} \quad (20e)$$

Now consider two special cases. In the first special case,  $\mathbf{a}_1 = \mathbf{a}_2$  but there is unequal variance  $\sigma_1^2 \neq \sigma_2^2$ . That is, a target is detected in the same direction but at different ranges. It is easy to verify that (20a) becomes:

$$(\mathbf{I} + \bar{\sigma}^{-2} \mathbf{a}_1 \mathbf{a}_1^T)^{-1} = \mathbf{I} - \bar{\gamma} \mathbf{a}_1 \mathbf{a}_1^T \quad (21a)$$

where

$$\bar{\sigma}^{-2} = \sigma_1^{-2} + \sigma_2^{-2} \quad (21b)$$

$$\bar{\gamma} = \frac{1}{\bar{\sigma}^2 + 1} = \frac{\sigma_1^2 + \sigma_2^2}{\sigma_1^2 + \sigma_2^2 + \sigma_1^2 \sigma_2^2} \quad (21c)$$

If  $\sigma_1^2 = \sigma_2^2$ , then  $\bar{\sigma}^2 = \sigma_1^2 / 2$  for an additional update. This is equivalent to reducing the measurement error variance by  $n$  with  $n$  additional updates. The corresponding eigenvalue decreases according to  $1/(n+1)$  for unity variance ( $\sigma^2 = 1$ ). The evaluation of continuously updated covariance is similar to running the covariance update equation of a Kalman filter (i.e., the Riccati equation).

In the second special case,  $\mathbf{a}_1 \perp \mathbf{a}_2$ , that is, they are perpendicular to each other. Then  $\rho = 0$  in (20b) and  $\gamma = 1$  in (20e) and (20a) becomes:

$$(\mathbf{I} + \sigma_1^{-2} \mathbf{a}_1 \mathbf{a}_1^T + \sigma_2^{-2} \mathbf{a}_2 \mathbf{a}_2^T)^{-1} = \mathbf{I} - \gamma_1 \mathbf{a}_1 \mathbf{a}_1^T - \gamma_2 \mathbf{a}_2 \mathbf{a}_2^T \quad (22)$$

It is easy to verify that (22) has the following eigenvalues and eigenvectors:

$$\mathbf{\Lambda} = \text{diag}([1 - \gamma_1 \quad 1 - \gamma_2]) \quad (23a)$$

$$\mathbf{V} = [\mathbf{a}_1 \quad \mathbf{a}_2] \quad (23b)$$

This indicates that for two orthogonal LOS vectors, simultaneous update with two orthogonal sensors is equivalent to two independent updates in terms of the final error ellipse and their eigen-structure.

For the general case with two simultaneous LOS updates, the updated covariance is given by (20). The calculation of its eigenvalues and eigenvectors is rather involved except for the two special cases given in (21) and (22). The following simulation is used to analyze the general eigenvalues and eigenvectors.

Again let the initial covariance be a unit matrix,  $\mathbf{P}_0 = \text{diag}([1, 1])$ . We fix the first LOS vector at  $\theta_1 = 30^\circ$  with  $\mathbf{R}_1 = 1$ . We then vary the second LOS vector  $\theta_2$  from  $0^\circ$  to

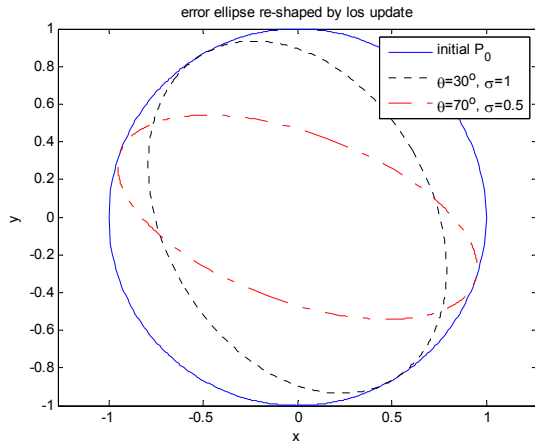


Fig. 2 Update of Unit Circle with Different  $\sigma$  and  $\theta$

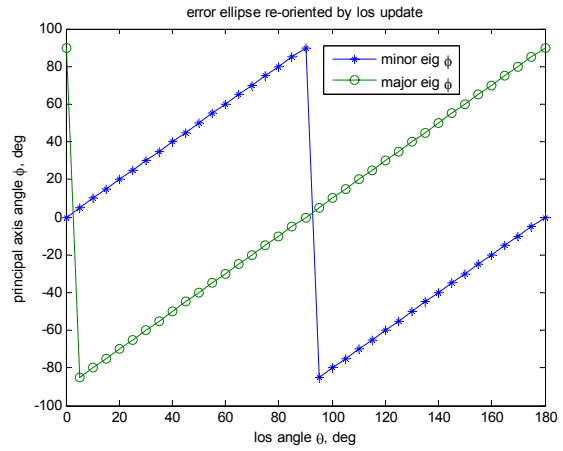


Fig. 3 Eigenvector Directions  $\phi$  vs. LOS Angle  $\theta$

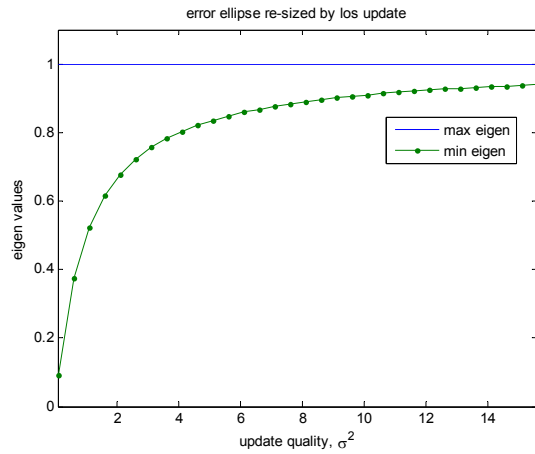


Fig. 4 Eigenvalues vs. Sensor Quality  $\sigma$

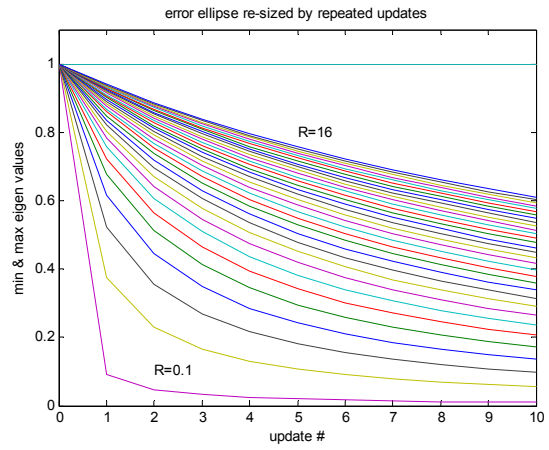


Fig. 5 Eigenvalues vs. Number of Updates

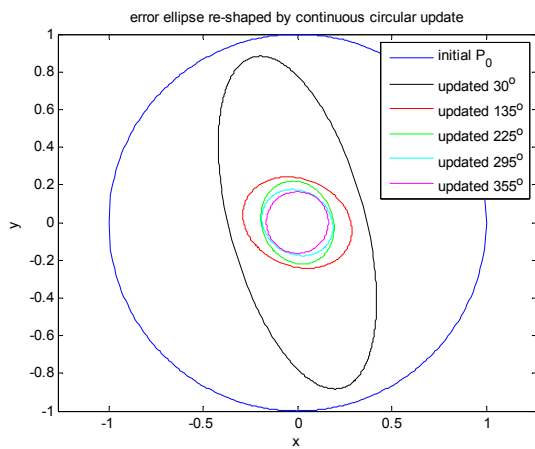


Fig. 6 Errors over Circular Updates

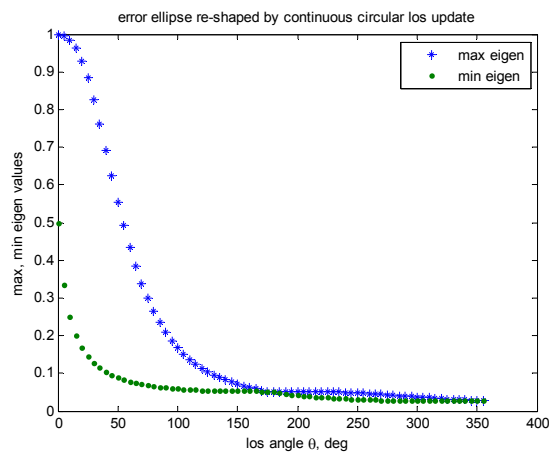


Fig. 7 Eigenvalues

180° and  $\mathbf{R}_2$  from 0.1 to 10. The major and minor eigenvalues as a function of  $\theta_2$  for different  $\mathbf{R}_2$  are showed in Figs. 8 and 9, respectively. Since  $\theta_1 = 30^\circ$ , the max and min values for both major and minor eigenvalues appear at  $\theta_2 = 30^\circ$  and  $\theta_2 = 120^\circ$ , respectively, which represent the two special cases given in (18) for  $\Delta\theta = \theta_2 - \theta_1 = 0^\circ$  and in (19) for  $\Delta\theta = \theta_2 - \theta_1 = 90^\circ$ .

Again with the first LOS vector fixed at  $\theta_1 = 30^\circ$  with  $\mathbf{R}_1 = 1$ , Figs. 10 and 11 show the major and minor eigenvector angles as the second LOS vector  $\theta_2$  varies from  $0^\circ$  to  $180^\circ$  and  $\mathbf{R}_2$  from 0.1 to 10. The two eigenvector angles have the same shapes except that they are off by  $90^\circ$ . For small  $\mathbf{R}_2$ , the second update dominates. As a result, the minor eigenvector points in this LOS direction and the major eigenvector is perpendicular to it.

For large  $\mathbf{R}_2$ , the second update becomes inconsequential and the first update dominates. That is why the curves remain close to  $\theta_1$  as  $\theta_2$  varies its value.

It is interesting to note the curves for  $\mathbf{R}_2 = \mathbf{R}_1$  seemly have a jump of  $90^\circ$  at  $\theta_2 = 120^\circ$  or  $\theta_2 - \theta_1 = 90^\circ$ . This is actually due to the switch of labeling of major and minor for the same eigenvectors. This is best illustrated in Fig. 12 for eigenvalues and Fig. 13 for eigenvectors for  $\mathbf{R}_2 = \mathbf{R}_1$  as a function of  $\theta_2$ .

As shown in Figs. 10 and 11, when  $\mathbf{R}_2$  and  $\mathbf{R}_1$  are comparable, the minor eigenvector angle lies between  $\theta_1$  and  $\theta_2$ . As the second LOS vector  $\theta_2$  moves away from the first LOS vector  $\theta_1$ , the minor eigenvector also moves away from  $\theta_1$ . But the eigenvector angular displacement lags that of  $\theta_2$  and stays somewhere between  $\theta_1$  and  $\theta_2$ .

Based on the simulation results, heuristic curves are shown in Fig. 14 for analysis and design. Fig 14(a) shows the approximate eigenvalues as a function of angular separation between the two LOS vectors. Fig 14(b) shows the approximate eigenvector angles as a function of angular separation between the two LOS vectors. Linear interpolation can be used to find the eigenvalues and eigenvector angles. In the figures, the effects of  $\mathbf{R}_1$  and  $\mathbf{R}_2$  are ignored but could be added with different curves in the same plot.

For an arbitrary covariance matrix  $\mathbf{A}$  and its inverse  $\mathbf{A}^{-1}$ , the eigen-decomposition is written as:

$$\mathbf{A} = \mathbf{U}\mathbf{\Lambda}\mathbf{U}^T \quad (24a)$$

$$\mathbf{A}^{-1} = \mathbf{U}\mathbf{\Lambda}^{-1}\mathbf{U}^T \quad (24b)$$

where

$$\mathbf{U} = [\mathbf{u}_1 \quad \cdots \quad \mathbf{u}_n] \quad (24c)$$

$$\mathbf{\Lambda} = \text{diag}([\lambda_1 \quad \cdots \quad \lambda_n]) \quad (24d)$$

$$\mathbf{\Lambda}^{-1} = \text{diag}([\lambda_1^{-1} \quad \cdots \quad \lambda_n^{-1}]) \quad (24e)$$

are the eigenvectors, eigenvalues, and inverse eigenvalues, respectively.

The matrix  $\mathbf{A}$  and its inverse  $\mathbf{A}^{-1}$  can be further written as:

$$\mathbf{A} = \sum_{i=1}^n \lambda_i \mathbf{u}_i \mathbf{u}_i^T \quad (25a)$$

$$\mathbf{A}^{-1} = \sum_{i=1}^n \lambda_i^{-1} \mathbf{u}_i \mathbf{u}_i^T \quad (25b)$$

Since the eigenvectors are orthonormal, they can be considered as the LOS vectors as in (22). As a result, the update of a unity circle with a covariance matrix (or a full rank observation matrix) can be readily obtained from (23), leading to the updated ellipse, which is re-oriented by the original eigenvectors (23b) but re-sized by the updated eigenvalues (23a). This thus provides a theoretical justification of our intuition about LOS updates, a geometrical interpretation of combining two ellipses, and a computational procedure for fusing them.

Since the trace of a matrix is the sum of its eigenvalues, we can evaluate the geometric dilution of precision (GDOP) directly from eigenvalues. For the case of updating with two LOS vectors where  $\theta_1 = 30^\circ$  and  $\mathbf{R}_1 = 1$ , Figure 15 shows the traces as a function of  $\theta_2$  for different  $\mathbf{R}_2$ . When  $\theta_2 = \theta_1$ , the trace is  $2 - \bar{\gamma}$ , which is the largest value. The smallest value occurs at  $\theta_2 - \theta_1 = 90^\circ$ , which is  $2 - \gamma_1 - \gamma_2$ . At other  $\theta_2$ , the trace lies in between following a sinusoidal curve. Fig. 16 is a linear approximation. For large  $\mathbf{R}$ , the trace does not change much with  $\theta$ . But it is significant for small  $\mathbf{R}$ . As shown in Fig. 15, the change in trace over  $\Delta\theta = 90^\circ$  is about the same for  $\mathbf{R}_2 = 0.1$  to 10 with  $\mathbf{R}_1 = 1$ . This is a tradeoff between assigning sensors with good quality vs. with good geometry over different time horizons.

The above analysis has been applied to the general case with an arbitrary initial error covariance [11]. Its relationship with GDOP [13] as well as geometric measure of merits (GMOM) [4] is presented in the context of sensor resource management for layered sensing [12].

## 4 Conclusions

In this paper, the use of range and bearing measurements for target positioning and tracking was investigated from the geometric point of view. As a scaling factor to the measurement prediction error vector, the observation matrix was shown to be made of line of sight (LOS) vectors from ranging sensors to target and unit vectors perpendicular to the LOS scaled by range from bearing-only sensors. As shown, the LOS vectors together with the sensor measurement error covariance determine the eigenstructure of position estimation error covariance, shaping the error ellipses. This geometric insight into target positioning and tracking with range and bearing measurements is helpful in designing an efficient resource management strategy for distributed sensors.

## Acknowledgements

Research supported in part under Contracts No. FA8650-05-C-1808 and FA8650-08-C-1407, which are gratefully acknowledged.

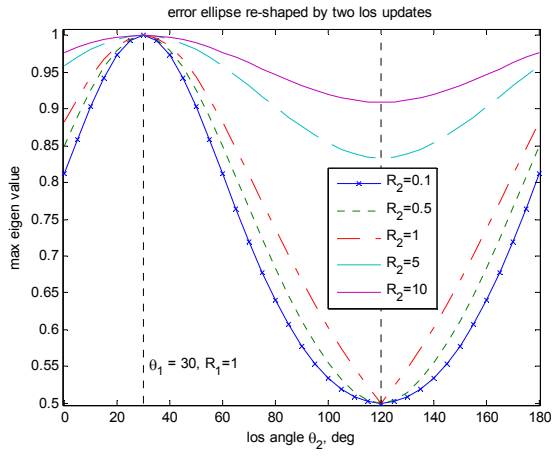


Fig. 8 Max Eigen over  $\Delta\theta$  for Different  $\sigma$

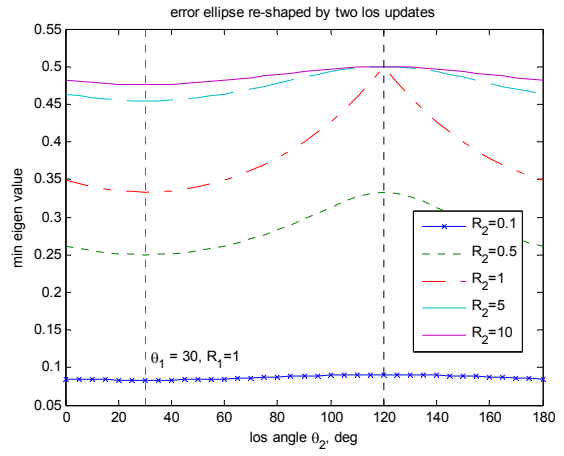


Fig. 9 Min Eigen over  $\Delta\theta$  for Different  $\sigma$

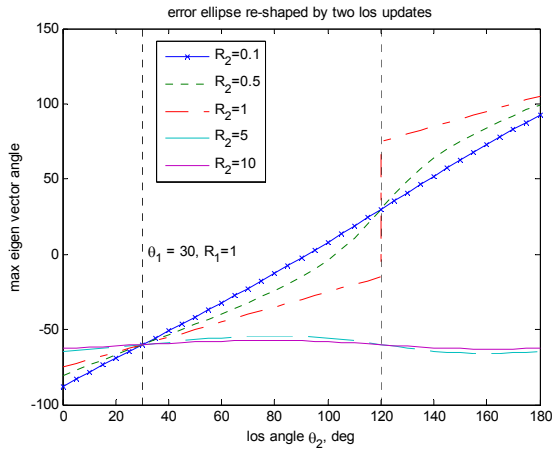


Fig. 10 Max Eigenvector over  $\Delta\theta$  for Different  $\sigma$

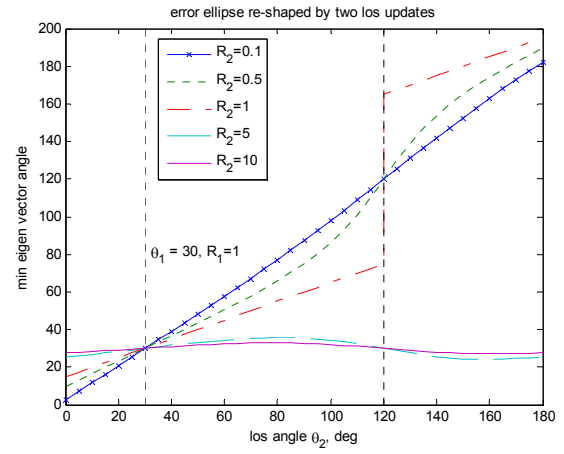


Fig. 11 Min Eigenvector over  $\Delta\theta$  for Different  $\sigma$

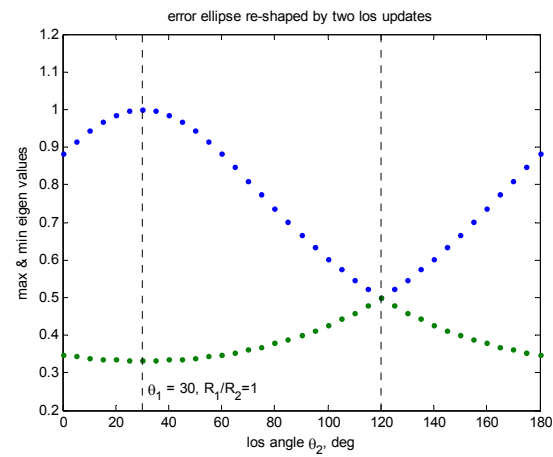


Fig. 12 Max and Min Eigenvalues over  $\Delta\theta$

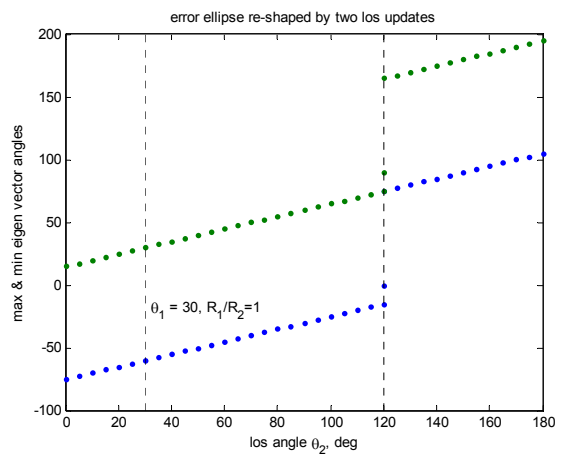
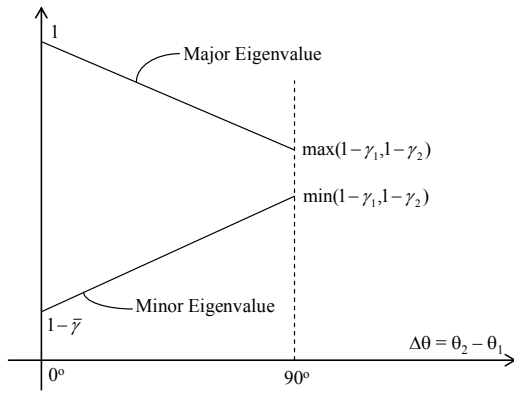
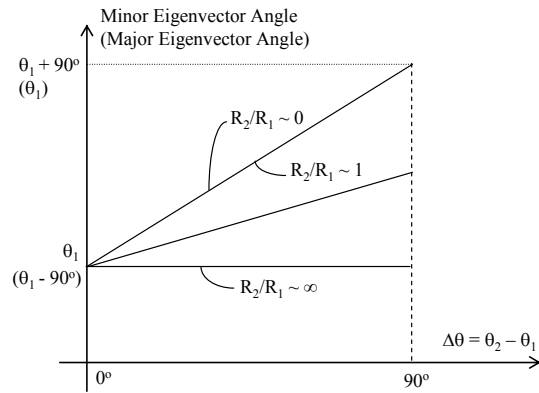


Fig. 13 Max and Min Eigenvectors over  $\Delta\theta$



(a) Approximation for Eigenvalues



(b) Approximation for Eigenvector

Figure 14 Linear Interpolation for Eigenvalues and Eigenvector as a Function of  $\Delta\theta$

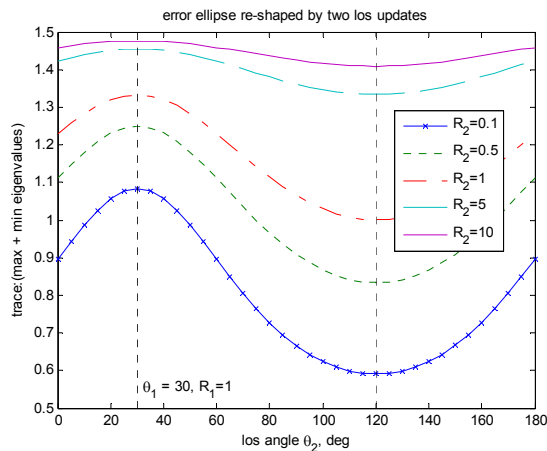


Fig. 15 Trace vs.  $\Delta\theta$  for Different  $\sigma$

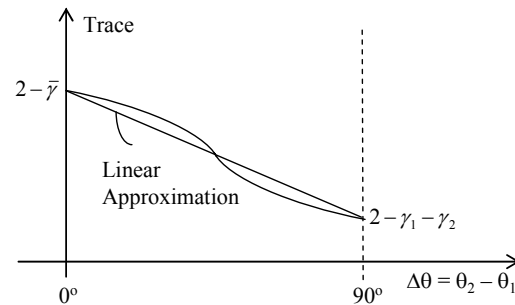


Fig. 16 Approximation for Trace

## References

- [1] Y. Bar-Shalom and X.R. Li, *Multitarget-Multisensor Tracking: Principles and Techniques*, YBS Publishing, Storrs, CT, 1995.
- [2] S. Blackman and R. Popoli, *Design and Analysis of Modern Tracking Systems*, Artech House, Boston, 1999.
- [3] A. Farina and F.A. Studer, *Radar Data Processing* (Vol. I & II), Wiley, New York, 1985.
- [4] I. Kadar, "Optimum Geometry Selection for Sensor Fusion," *Proc. SPIE Vol. 3374, p. 96-107, Signal Processing, Sensor Fusion, and Target Recognition VII*, Ivan Kadar (Ed.), April 1998.
- [5] I. Kadar, E. Blasch, and C. Yang, "Invited Panel Discussion: Issues and Challenges in Model-Based Performance Assessment of Multi-Target Trackers," *Proc. of SPIE Defense and Security 2008: Signal Processing, Sensor Fusion, and Target Recognition XVII*, Orlando, FL, March 2008.
- [6] B. Kahler and E. Blasch, "Sensor Management Fusion Using Operating Conditions," *Proc. of IEEE NAECON'08*, Dayton, OH, July 2008.
- [7] P. Maybeck, *Stochastic Models, Estimation, and Control*, Volume 1, Academic Press, Inc, 1979.
- [8] S.U. Pillai, K.Y. Li, and B. Himed, *Space Based Radar: Theory & Applications*, McGraw Hill, New York, 2008.
- [9] R. Popoli, "The Sensor Management Imperative", Ch.10 in *Multitarget-Multisensor Tracking: Applications and Advances*, Vol.2, Y. Bar-Shalom (Ed.), 325-392, Artech House, Norwood, MA, 1999.
- [10] B. Ristic, S. Arullampalam, & N. Gordon, *Beyond the Kalman Filter: Particle filters for tracking applications*, Artech House, 2004.
- [11] C. Yang, *Performance Monitoring and Prediction for Active Management of Distributed Sensors Fusion in Target Tracking*, Status Report No. 4 (FA8650-08-C-1407), November 2008.
- [12] C. Yang, I. Kadar, and E. Blasch, "Performance-Driven Resource Management in Layered Sensing," *Fusion'2009*, Seattle, WA, July 2009.
- [13] R. Yarlagadda, I. Ali, N. Al-Dhahir, and J. Hershey, "GPS GDOP Metric," *IEE Proc. Radar, Sonar Navig*, 147(5), Oct. 2000.
- [14] A. Kelly, "Precision Dilution in Triangulation Based Mobile Robot Position Estimation," *Intelligent Autonomous Systems*, Amsterdam, 2003.
- [15] I. Kadar, "Passive Multisensor Multitarget Feature-Aided Unconstrained Tracking: A Geometric Perspective," *Fusion2000*, July 2000.
- [16] M. Kihara and T. Okada, "A Satellite Selection Method and Accuracy for the Global Positioning System," *Navigation: Journal of the ION*, 31(1), 1984.